



PERIODIC NUCLEATION SOLUTIONS OF THE REAL GINZBURG–LANDAU EQUATION IN A FINITE BOX

M. ARGENTINA

*Centro de Física No Lineal y Sistemas Complejos de Santiago
Casilla 27122, Santiago, Chile*

O. DESCALZI

*Facultad de Ingeniería. Universidad de los Andes
Av. San Carlos de Apoquindo 2200, Santiago, Chile
orazioid@uandes.cl*

E. TIRAPEGUI

*Departamento de Física, F.C.F.M. Universidad de Chile
Casilla 487-3, Santiago, Chile*

Received August 9, 2001; Revised October 11, 2001

We study the stationary solutions of the real Ginzburg–Landau equation with periodic boundary conditions in a finite box. We show explicitly how to construct nucleation solutions allowing transitions between stable plane waves.

Keywords: Nucleation solutions; real Ginzburg–Landau equation; Eckhaus instability; Lyapounov functional.

1. Introduction

In the vicinity of the threshold of a continuous pattern-forming instability a description of the basic periodic solution and its slow modulations is possible by perturbation theory [Newell & Whitehead, 1969; Segel, 1969; Stuart & Di Prima, 1978]. For quasi-one-dimensional, stationary, and periodic patterns formed from an unstructured state through a continuous soft-mode finite- q instability, a description in terms of $A(x, t)$ satisfying the real Ginzburg–Landau equation is as follows

$$\partial_t A = A - |A|^2 A + \partial_{xx} A, \quad (1)$$

where the complex amplitude $A(x, t)$ is a function of the slow space and time variables, x and t , respectively. This equation is the normal form [Elphick *et al.*, 1987] when an eigenvalue crosses the real axis at the origin for a finite wave number.

We shall consider here periodic boundary conditions $A(0, t) = A(L, t)$. Equation (1) can be written as $\partial_t A = -1/2\delta\Phi/\delta\bar{A}$ with $\Phi = -2 \int_0^L (|A|^2 - 1/2|A|^4 - |\partial_x A|^2) dx$. The dynamical system (1) admits stable and unstable stationary plane wave solutions and homogeneous stationary solutions. Moreover there exist stationary nucleation solutions which play an important role in the calculation of the smallest perturbation which induces the transition between two given stable plane waves. This perturbation is related to the codimension-one unstable manifold of the unstable inhomogeneous solution. As usual the stationary solutions of (1) are also extrema of the Lyapounov functional Φ . Earlier works [Langer & Ambegaokar, 1967; McCumber & Halperin, 1970; Tribelsky *et al.*, 1991; Graham & Tel, 1990; Kramer & Zimmermann, 1985] have been mainly devoted to study such solutions in an infinite box. Nevertheless in [Tuckermann & Barkley, 1990] was reported the

scenario of the Eckhaus bifurcation in a finite domain. Our work generalizes the above results and permits to construct explicitly the nucleation stationary solutions in a finite box.

2. Stationary Solutions in a Finite Box

2.1. Nucleation solutions

In polar coordinates, $A = r \exp(i\varphi)$, Eq. (1) takes the form

$$\begin{aligned} r_t &= r - r^3 - r\varphi_x^2 + r_{xx}; \\ r\varphi_t &= 2r_x\varphi_x + r\varphi_{xx}. \end{aligned} \tag{2}$$

The stationary solutions of Eq. (2) correspond to $r_t = \varphi_t = 0$. The homogeneous ones to $r = 0$ (unstable) and $r = 1$ (stable), $\varphi = \varphi_0$ (arbitrary constant). The stationary plane wave solutions correspond to $r = \sqrt{1 - q^2}$, $\varphi_x = q$ (arbitrary constant such that $q^2 \leq 1$). To obtain the nucleation solutions we integrate Eq. (2) using two first integrals, namely, E and J , corresponding to the energy and angular momentum in a mechanical analogous:

$$E = r_x^2 + U(r, J); \quad J = r^2\varphi_x, \tag{3}$$

where $U(r, J) = r^2 - r^4/2 + J^2/r^2$. Bounded solutions demand $J^2 \leq 4/27$.

If r_a and r_b correspond to plane waves then $r_a = \sqrt{1 - q_a^2}$ and $r_b = \sqrt{1 - q_b^2}$, where q_a and q_b are solutions of $J = q(1 - q^2)$. Denoting r_1, r_2 and r_3 ($r_1 \leq r_2 \leq r_3$) as the roots of the equation $E = U(r, J)$ we get $r(x)$ in terms of the Jacobi

elliptic function $\text{cn}(u|m)$

$$\begin{aligned} r(x) &= \left[r_2^2 + (r_1^2 - r_2^2)\text{cn}^2 \right. \\ &\quad \left. \times \left(\sqrt{r_3^2 - r_1^2} \frac{x}{\sqrt{2}} \left| \frac{r_2^2 - r_1^2}{r_3^2 - r_1^2} \right| \right) \right]^{\frac{1}{2}}, \end{aligned} \tag{4}$$

and the phase $\varphi(x)$ in terms of the incomplete elliptic integral of the third kind $\Pi(n; \phi|m)$

$$\begin{aligned} \varphi(x) &= \frac{r_2 r_3 \text{sign}(x)}{r_1 \sqrt{r_2^2 - r_1^2}} \Pi \left(1 - \frac{r_3^2}{r_1^2}; \right. \\ &\quad \left. \arcsin \sqrt{\frac{r^2(x) - r_1^2}{r_3^2 - r_1^2}} \left| \frac{r_3^2 - r_1^2}{r_2^2 - r_1^2} \right| \right). \end{aligned} \tag{5}$$

The amplitude $r(x)$ has period

$$L = \frac{2\sqrt{2}}{\sqrt{r_3^2 - r_1^2}} K \left(\frac{r_1^2 - r_2^2}{r_1^2 - r_3^2} \right) = \tilde{\psi}^{(1)}(E, J), \tag{6}$$

where $K(m)$ is the complete elliptic integral of the first kind. The phase variation in this period is

$$\begin{aligned} \Delta\varphi &= \varphi \left(\frac{L}{2} \right) - \varphi \left(-\frac{L}{2} \right) \\ &= \frac{2r_2 r_3}{r_1 \sqrt{r_3^2 - r_1^2}} \Pi \left(1 - \frac{r_2^2}{r_1^2} \left| \frac{r_2^2 - r_1^2}{r_3^2 - r_1^2} \right| \right) \\ &= \tilde{\psi}^{(2)}(E, J), \end{aligned} \tag{7}$$

where $\Pi(n|m)$ is the complete elliptic integral of the third kind.

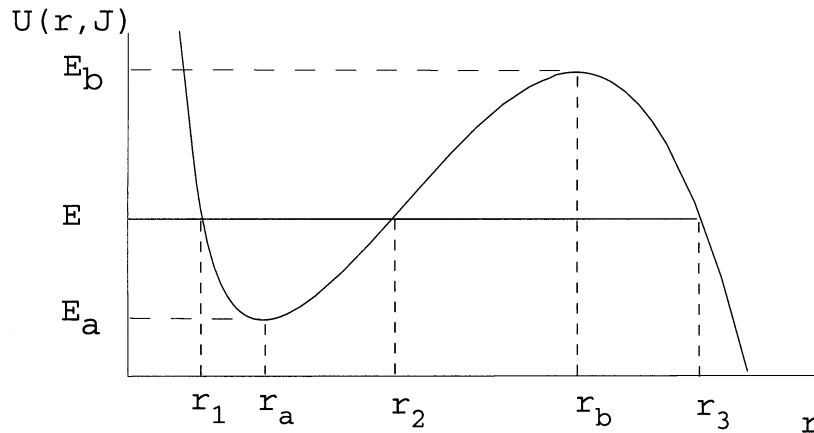


Fig. 1. The potential energy $U(r, J)$, in the mechanical analogous, is intersected by the energy E in r_1, r_2 and r_3 . E_a and E_b are the minimal and the maximal allowed energies for bounded solutions.

The relations between r_1, r_2 and r_3 with E and J (see Fig. 1) are given by

$$\begin{aligned} r_1^2 + r_2^2 + r_3^2 &= 2, \\ r_1^2 r_3^2 + r_2^2 r_3^2 + r_1^2 r_2^2 &= 2E, \\ r_1^2 r_2^2 r_3^2 &= 2J^2. \end{aligned} \tag{8}$$

Through the relation $J = q_b(1 - q_b^2)$ we can express L and $\Delta\varphi$ in terms of q_b and we put $\psi^{(j)}(E, q_b) \equiv \tilde{\psi}^{(j)}(E, J)$, $j = 1, 2$. For fixed J (or q_b) we see that for each value of E , $E_{\min} = E_a < E < E_{\max} = E_b$, there corresponds a value L of the period such that $L_{\min} < L < \infty$. Once L is given we can calculate the values of (r_1, r_2, r_3) and then $r(x)$ and $\varphi(x)$ are completely determined. We must still impose, due to the periodic boundary conditions, that $\Delta\varphi = 2n\pi$, where n is an integer. We can write then from (6) and (7) the two relations

$$L = \psi^{(1)}(E, q_b); \quad \Delta\varphi = \psi^{(2)}(E, q_b) = 2n\pi. \tag{9}$$

Eliminating E we obtain the family of curves

$$L = \psi(q_b, n), \tag{10}$$

which we shall determine in what follows. The period L given by Eq. (6) diverges logarithmically when the argument of the complete elliptic integral of the first kind tends to unity. We can find analytical results for energies near the maximal allowed energy E_b . The remarkable point is, as we shall see, that solutions with periods of the order 10 or higher can be described with negligible errors in this limit.

Putting $\delta = E_b - E$ we can expand, for q_b fixed, the values of (r_1, r_2, r_3) for small δ . One has

$$\begin{aligned} r_1^2 &= 2q_b^2 + \frac{4q_b^2\delta}{(1 - 3q_b^2)^2} + O(\delta^2), \\ r_2^2 &= 1 - q_b^2 - \sqrt{2} \left[\frac{1 - q_b^2}{1 - 3q_b^2} \right]^{\frac{1}{2}} \delta^{\frac{1}{2}} \\ &\quad - \frac{2q_b^2\delta}{(1 - 3q_b^2)^2} + O(\delta^{\frac{3}{2}}), \\ r_3^2 &= 1 - q_b^2 + \sqrt{2} \left[\frac{1 - q_b^2}{1 - 3q_b^2} \right]^{\frac{1}{2}} \delta^{\frac{1}{2}} \\ &\quad - \frac{2q_b^2\delta}{(1 - 3q_b^2)^2} + O(\delta^{\frac{3}{2}}). \end{aligned} \tag{11}$$

Inserting these values in Eqs. (6) and (7) we obtain

$$\begin{aligned} L &= \frac{\sqrt{2}}{2(1 - 3q_b^2)^{\frac{1}{2}}} \ln \left[\frac{32(1 - 3q_b^2)^3}{(1 - q_b^2)\delta} \right] + O(\delta), \\ \Delta\varphi &= \pi - 2 \arcsin \left[\frac{\sqrt{2}q_b}{\sqrt{1 - q_b^2}} \right] \\ &\quad + \frac{q_b\sqrt{2}}{2(1 - 3q_b^2)^{\frac{1}{2}}} \ln \left[\frac{32(1 - 3q_b^2)^3}{(1 - q_b^2)\delta} \right] + O(\delta). \end{aligned} \tag{12}$$

We have then, in the lowest order in δ , the following relation between $L, \Delta\varphi$ and q_b (we remark that the exact relation between these variables is obtained eliminating E between the two Eqs. (9))

$$\Delta\varphi = \pi - 2 \arcsin \left[\frac{\sqrt{2}q_b}{\sqrt{1 - q_b^2}} \right] + q_b L + O(\delta). \tag{13}$$

Using $\Delta\varphi = 2n\pi$, where n is the phase winding number, we obtain a lowest order approximation for the curves (10)

$$\begin{aligned} L &= \psi(q_b, n) \\ &= \frac{1}{q_b} \left[(2n - 1)\pi + 2 \arcsin \left(\frac{\sqrt{2}q_b}{\sqrt{1 - q_b^2}} \right) \right] + O(\delta), \end{aligned} \tag{14}$$

which turns out to be extremely accurate in its region of validity. We can write (14) in the equivalent form

$$\frac{\sqrt{2}q_b}{\sqrt{1 - q_b^2}} = \cos \left(\frac{q_b L}{2} \right) \cos n\pi + O(\delta). \tag{15}$$

The values of L are limited from below by the minimum L reached for each q_b . L_{\min} is given by Eq. (6) in the limit $r_1 \rightarrow r_2 \rightarrow r_a$, where the solutions become harmonic.

$$L_{\min} = \frac{2\sqrt{2}}{\sqrt{r_3^2 - r_1^2}} K(0) = \frac{\sqrt{2}\pi}{\sqrt{3q_a^2 - 1}}. \tag{16}$$

Since $q_a = 1/2(-q_b + \sqrt{4 - 3q_b^2})$ we finally obtain the exact expression for L_{\min} in terms of q_b

$$L_{\min} = \frac{2\pi}{\sqrt{4 - 3q_b^2 - 3q_b\sqrt{4 - 3q_b^2}}}. \tag{17}$$

In Fig. 2 we plot the curves $L = \psi(q_b, n)$ [see (10)] in the approximation (14) for different phase winding numbers n (dashed curves) and the length for plane

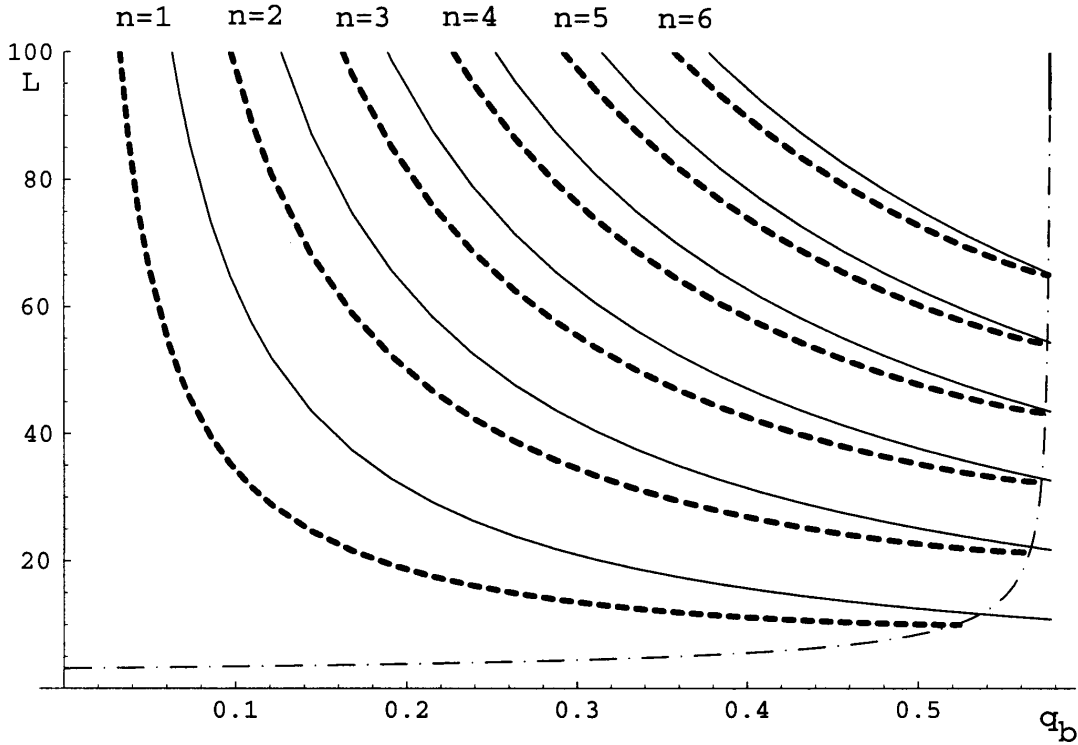


Fig. 2. Plot of L versus q_b for different phase winding numbers (dashed curves) and for plane waves (continuous curves). The dot-dashed line is the curve L_{\min} .

waves with wave number q_b (continuous curves), i.e. $L = 2\pi n/q_b$. The former curves are bounded from below by the curve L_{\min} given by (17).

Thus for a fixed value of L , the length of the system, and n , the phase winding number, we can determine q_b from Eq. (14). The value of δ , which is directly related to the error of the perturbative expansion, is given in the dominant order by Eq. (12)

$$\delta = 32 \frac{(1 - 3q_b^2)^3}{(1 - q_b^2)} e^{-L\sqrt{2}\sqrt{1-3q_b^2}}. \quad (18)$$

Notice the exponential decrease with L of δ . We can estimate from this expression that the error is negligible for $L > 10$. We can now use this last result in (11) and then determine the corresponding expressions for $r(x)$ and $\varphi(x)$ given by (4) and (5) in this approximation. We obtain $r = r(x, L, q_b)$, $\varphi = \varphi(x, L, q_b)$, and if we calculate $\Delta\varphi = 2\pi n = \varphi(x = L, L, q_b) - \varphi(x = 0, L, q_b)$ we recuperate expression (13).

With our general results we can get an interesting limit, namely, the case when the length of the system becomes ∞ . In this limit $r_2 \rightarrow r_3 \rightarrow r_b =$

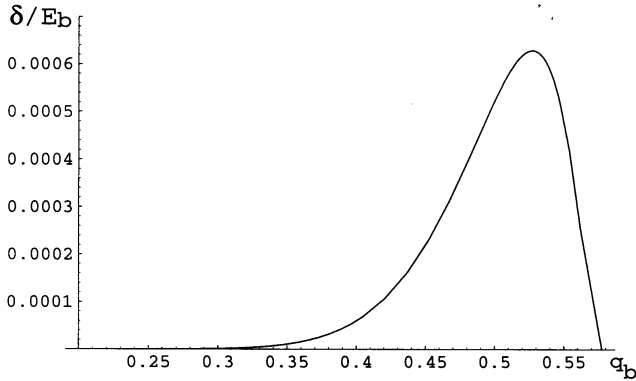
$\sqrt{1 - q_b^2}$. It is easy to show that Eq. (4) becomes

$$r(x) = \left[2q_b^2 + (1 - 3q_b^2) \tanh^2 \left(\sqrt{1 - 3q_b^2} \frac{x}{\sqrt{2}} \right) \right]^{\frac{1}{2}}, \quad (19)$$

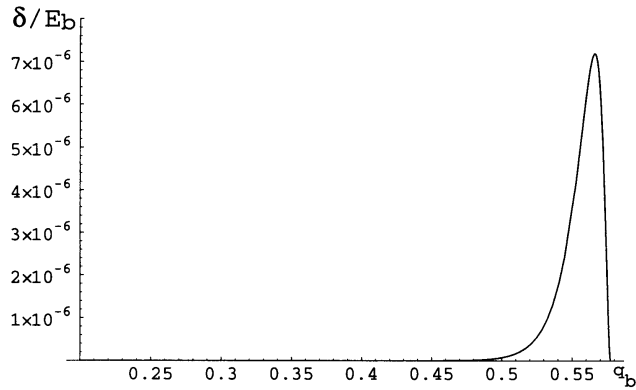
and Eq. (5) reads

$$\begin{aligned} \varphi(x) = & q_b x \\ & + \arctan \left[\frac{\sqrt{1 - 3q_b^2}}{\sqrt{2}q_b} \tanh \left(\sqrt{1 - 3q_b^2} \frac{x}{\sqrt{2}} \right) \right]. \end{aligned} \quad (20)$$

The above calculated function represents the saddle between a plane wave with wave number q_b and its neighbor in a system with length $L \rightarrow \infty$. This case has been largely studied in [Langer & Ambegaokar, 1967; McCumber & Halperin, 1970; Tribelsky *et al.*, 1991; Graham & Tel, 1990; Kramer & Zimmermann, 1985]. From a linear stability analysis of these solutions we can find two zero eigenvalues (the translational and phase symmetries), and the eigenvalues $\lambda_{\pm} = -1/2(1 + q_b^2) \pm \sqrt{1 - 4q_b^2 + 7q_b^4}$



(a)



(b)

Fig. 3. Plot of δ/E_b versus q_b . (a) Case $n = 1$. (b) Case $n = 2$.

for the localized discrete-eigenvalues solutions, with $\lambda_+ > 0$ giving the unstable direction.

It is also clear for us that Eq. (14) can be derived from Eq. (20) by making $L \gg 1$, but without any control of the error done in such approximation. This error is estimated here. The functions $L = \psi(q_b, n)$ in Eq. (14) have been calculated neglecting terms $O(\delta)$. In order to obtain an impression of the exactness of our curves, drawn in Fig. 2, we proceed to evaluate δ as a function of q_b . Replacing L given by Eq. (14) in Eq. (18) we get

$$\delta = 32 \frac{(1 - 3q_b^2)^3}{(1 - q_b^2)} \exp \left\{ -\sqrt{2} \sqrt{1 - 3q_b^2} \frac{1}{q_b} \left[(2n - 1)\pi + 2 \arcsin \left(\frac{\sqrt{2}q_b}{\sqrt{1 - q_b^2}} \right) \right] \right\}. \tag{21}$$

Figures 3(a) and 3(b) show a plot of δ/E_b versus q_b for $n = 1$ and $n = 2$, respectively.

To analyze in more detail the intersection between the curve $\psi(q_b, n)$ and the curve L_{\min} , where the error is maximum, we expand Eqs. (8) in terms of $\varepsilon = E - E_a$ (see Fig. 1). Thus r_1^2 , r_2^2 and r_3^2 acquire the following form

$$\begin{aligned} r_1^2 &= 1 - q_a^2 - \sqrt{2} \left[\frac{1 - q_a^2}{3q_a^2 - 1} \right]^{\frac{1}{2}} \varepsilon^{\frac{1}{2}} \\ &\quad + \frac{2q_a^2 \varepsilon}{(1 - 3q_a^2)^2} + O(\varepsilon^{\frac{3}{2}}), \\ r_2^2 &= 1 - q_a^2 + \sqrt{2} \left[\frac{1 - q_a^2}{3q_a^2 - 1} \right]^{\frac{1}{2}} \varepsilon^{\frac{1}{2}} \\ &\quad + \frac{2q_a^2 \varepsilon}{(1 - 3q_a^2)^2} + O(\varepsilon^{\frac{3}{2}}), \\ r_3^2 &= 2q_a^2 - \frac{4q_a^2 \varepsilon}{(1 - 3q_a^2)^2} + O(\varepsilon^2). \end{aligned} \tag{22}$$

Inserting these values in Eqs. (6) and (7) we get an expression for L in terms of q_a and ε

$$L = \frac{\pi\sqrt{2}}{\sqrt{3q_a^2 - 1}} + \frac{3\pi(1 + 7q_a^2)\varepsilon}{4\sqrt{2}(3q_a^2 - 1)^{\frac{7}{2}}} + O(\varepsilon^2), \tag{23}$$

and a relation between $\Delta\varphi$, q_a and ε

$$\Delta\varphi = \frac{\pi\sqrt{2}q_a}{\sqrt{3q_a^2 - 1}} + \frac{15\pi\sqrt{2}q_a(1 - q_a^2)\varepsilon}{8(3q_a^2 - 1)^{\frac{7}{2}}} + O(\varepsilon^2). \tag{24}$$

Once again due to the periodic boundary conditions one must have $\Delta\varphi = 2n\pi$, where n is the phase winding number. Using this condition and $\varepsilon = 0$, Eq. (24) has as solution $q_a^* = (\sqrt{2}n)/(\sqrt{6n^2 - 1})$. Moreover we can write q_a in terms of q_a^* and ε

$$q_a = q_a^* + \frac{15q_a^*(1 - q_a^{*2})}{8(1 - 3q_a^{*2})^2} \varepsilon + O(\varepsilon^2). \tag{25}$$

Considering that $q_b = 1/2(-q_a + \sqrt{4 - 3q_a^2})$ we obtain the point $(q_b^*, \psi(q_b^*, n))$ where the curve $\psi(q_b, n)$ intersects L_{\min}

$$\begin{aligned} q_b^* &= \frac{\sqrt{2}}{2\sqrt{6n^2 - 1}} (\sqrt{9n^2 - 2} - n); \\ \psi(q_b^*, n) &= \pi\sqrt{2}\sqrt{6n^2 - 1}. \end{aligned} \tag{26}$$

In the case $n = 1$, which is shown in Fig. 4, these curves intersect at $q_b^* = (\sqrt{7} - 1)/\sqrt{10} = 0.52043$ and $\psi(q_b^*, 1) = \pi\sqrt{10} = 9.93458$. Thus we can determine the nucleation solutions in the neighborhood of the point $(q_b^*, \psi(q_b^*, n))$

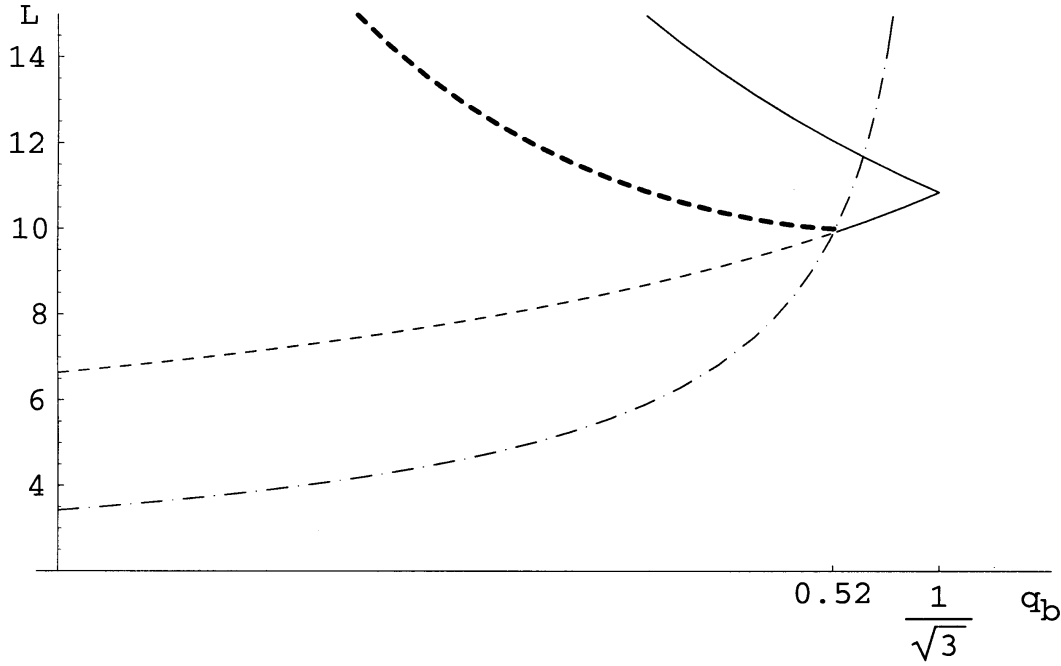


Fig. 4. The dark dashed line represents the nucleation function with phase winding number $n = 1$. The light dashed line stands for the unstable plane wave with phase winding number $n = 1$. The solid line stands for the stable plane wave with phase winding number $n = 1$. The dot-dashed line is the curve L_{\min} .

$$r(x) = \sqrt{1 - q_a^{*2}} - \frac{\cos(\sqrt{2}\sqrt{3q_a^{*2} - 1}x)}{\sqrt{2}\sqrt{3q_a^{*2} - 1}} \varepsilon^{\frac{1}{2}} + \frac{(3(1 - 4q_a^{*2} + 5q_a^{*4}) - (1 + q_a^{*2}) \cos(2\sqrt{2}\sqrt{3q_a^{*2} - 1}x))}{8(3q_a^{*2} - 1)^2 \sqrt{1 - q_a^{*2}}} \varepsilon + O(\varepsilon^{\frac{3}{2}}), \tag{27}$$

$$\varphi(x) = q_a^* x + \frac{q_a^* \sin(\sqrt{2}\sqrt{3q_a^{*2} - 1}x)}{(3q_a^{*2} - 1)\sqrt{1 - q_a^{*2}}} \varepsilon^{\frac{1}{2}} - \frac{q_a^*(5q_a^{*2} - 1)(3(q_a^{*2} - 1)\sqrt{3q_a^{*2} - 1}x + \sqrt{2} \sin(2\sqrt{2}\sqrt{3q_a^{*2} - 1}x))}{8(3q_a^{*2} - 1)^{\frac{5}{2}}(q_a^{*2} - 1)} \varepsilon + O(\varepsilon^{\frac{3}{2}}), \tag{28}$$

and the length of these solutions is given by

$$L = \frac{\pi\sqrt{2}}{\sqrt{3q_a^{*2} - 1}} + \frac{3\pi(5q_a^{*2} - 1)\varepsilon}{4\sqrt{2}(3q_a^{*2} - 1)^{\frac{5}{2}}} + O(\varepsilon^2). \tag{29}$$

A perturbative linear stability analysis of the above solutions gives us a spectrum with two zero eigenvalues (phase and translation symmetry), one positive eigenvalue $\lambda = (21n^2 - 9/2)\varepsilon$ and the rest negative eigenvalues.

2.2. Vortex solutions

Beside the homogeneous stationary solutions $r = 0$, $r = 1$; $\varphi = \varphi_0$, the plane waves and nucleation solu-

tions, Eqs. (2) accept vortex solutions when $J = 0$. In order to determine them we look for functions whose module vanishes at least at one space point x_0 where the phase can change by multiples of 2π .

Using Eqs. (4) and (8) we get

$$r(x) = r_2 \sqrt{\text{sn}^2\left(\frac{r_3 x}{\sqrt{2}} \middle| \frac{r_2^2}{r_3^2}\right)}, \tag{30}$$

$$\varphi(x) = \varphi_0 + 2n\pi H(x),$$

$$r_2^2 = 1 - \sqrt{1 - 2E},$$

$$r_3^2 = 1 + \sqrt{1 - 2E},$$

where $H(x)$ is the Heaviside function. To get bounded vortex solutions we have to demand $0 < E < 1/2$. The length of this function can be calculated by Eqs. (6) and (30)

$$L = \frac{2\sqrt{2}}{\sqrt{1 + \sqrt{1 - 2E}}} K \left(\frac{(1 - \sqrt{1 - 2E})^2}{2E} \right). \quad (31)$$

In order to have explicit expressions for $r(x)$ in terms of the length L we expand E in terms of $\eta = 1/2 - E$. Thus

$$\eta = 32e^{-\sqrt{2}L}. \quad (32)$$

Using this result we can write an explicit expression for the vortex solution in terms of the length L

$$r(x) = (1 - 4e^{-\frac{L}{\sqrt{2}}}) \times \sqrt{\operatorname{sn}^2 \left(\frac{(1 + 4e^{-\frac{L}{\sqrt{2}}})x}{\sqrt{2}} \middle| 1 - 16e^{-\frac{L}{\sqrt{2}}} \right)},$$

$$\varphi(x) = \varphi_0 + 2n\pi H(x). \quad (33)$$

A linear stability analysis of solution Eq. (30) yields that the spectrum of the linearized problem has two zero eigenvalues, one expected positive eigenvalue $\lambda = 1/2(2 - r_3^2)$ and the rest negative eigenvalues.

3. The Eckhaus Instability in a Finite Box

Every stationary solution constructed in the preceding section, which satisfies periodic boundary conditions becomes characterized by two parameters, namely, $J = q_a(1 - q_a^2) = q_b(1 - q_b^2)$ and E . Imposing periodic boundary conditions the length L becomes a function of q_b and n as it is shown in Eq. (10) and its approximate version (14).

For each q_b , provided that $0 \leq q_b \leq 1/\sqrt{3}$, there exist two plane waves with different wave numbers, namely, q_b and q_a . Therefore the two different plane waves have different lengths, namely, $L = 2\pi n/q_b$ and $L = 2\pi n/q_a$. When $q_b \rightarrow 1/\sqrt{3}$ both periods coincide and take the value $L = 2\pi n\sqrt{3}$.

Now let us analyze the stability of a plane wave $A_q = \sqrt{1 - q^2}e^{iqx}$ under a small perturbation bA_q , where b is a small periodic perturbation. Replacing $A = A_q(1 + b)$ in Eq. (1) we obtain the following linearized equation

$$\partial_t b = -(1 - q^2)(b + \bar{b}) + 2iq\partial_x b + \partial_{xx} b, \quad (34)$$

where \bar{b} is the complex conjugate of b . Writing $b = u + iv$ we get

$$\partial_t \begin{pmatrix} u \\ v \end{pmatrix} = \begin{pmatrix} -2(1 - q^2) + \partial_{xx} & -2q\partial_x \\ 2q\partial_x & \partial_{xx} \end{pmatrix} \begin{pmatrix} u \\ v \end{pmatrix}. \quad (35)$$

Replacing $\begin{pmatrix} u \\ v \end{pmatrix} = \begin{pmatrix} u_p \\ v_p \end{pmatrix} e^{\lambda t + ipx}$ in Eq. (35) the eigenvalue problem reduces to the analysis of the polynomial

$$\lambda^2 + 2\lambda(p^2 + 1 - q^2) + p^2(2 - 6q^2 + p^2) = 0. \quad (36)$$

If $p = 0$ there exist one marginal mode and one stable mode. If $p \neq 0$ the stability condition is

$$(2(1 - 3q^2) + p^2)p^2 > 0, \quad (37)$$

which is equivalent to

$$q^2 < \frac{1}{3} + \frac{p^2}{6}. \quad (38)$$

In a system with $L \rightarrow \infty$ the wave number p can take any value, in particular $p = 0$. In that case the stability condition would become the well known Eckhaus criterion for the stability of plane waves against long wavelength perturbations

$$q^2 < \frac{1}{3}. \quad (39)$$

But for systems in a finite box $p = 2m\pi/L$, $q = 2n\pi/L$, the stability criterion is obtained for the smallest accessible p , namely $p = 2\pi/L$. Therefore the stability condition given by Eq. (37) becomes

$$L > \pi\sqrt{2}\sqrt{6n^2 - 1}. \quad (40)$$

Notice that the critical point for the Eckhaus instability in a finite box coincides with the one just calculated in Eq. (26). This result is related to the saddle-node bifurcation with rotational symmetry derived in [Tuckermann & Barkley, 1990]. In Fig. 4 we represented the situation for solutions with phase winding number $n = 1$. There we see that for $L < 2\pi$ there is no plane wave. For $2\pi < L < \pi\sqrt{10}$ the existing plane wave is unstable against small perturbations according to Eq. (40). For $L > \pi\sqrt{10}$ we have an unstable nucleation solution and a stable plane wave.

4. The Lyapounov Functional

As we mentioned in the Introduction the real Ginzburg–Landau equation can be written in a gradient form

$$\partial_t A = -\frac{1}{2} \frac{\delta \Phi}{\delta \bar{A}}, \tag{41}$$

where the Lyapounov Functional Φ is given by

$$\Phi = -2 \int_0^L \left(|A|^2 - \frac{1}{2}|A|^4 - |\partial_x A|^2 \right) dx. \tag{42}$$

Taking into account the change of variables $(A, \bar{A}) \rightarrow (r, \varphi)$ and Eqs. (8) it is possible to obtain an explicit expression for Φ evaluated at the saddle function with phase winding number n and length L .

$$\begin{aligned} \Phi = & \frac{8\sqrt{2}}{3} \sqrt{r_2^2 - r_1^2} E \left(\arcsin \sqrt{\frac{r_2^2 - r_1^2}{r_3^2 - r_1^2}} \middle| \frac{r_3^2 - r_1^2}{r_2^2 - r_1^2} \right) \\ & + \frac{2\sqrt{2}}{3\sqrt{r_3^2 - r_1^2}} (r_1^2 r_3^2 + r_2^2 (r_1^2 + r_3^2 \\ & - 4)) K \left(\frac{r_2^2 - r_1^2}{r_3^2 - r_1^2} \right), \end{aligned} \tag{43}$$

where $E(\phi, m)$ is the incomplete elliptic integral of the second kind.

In the case of vortex functions the functional is given by

$$\begin{aligned} \Phi = & \frac{8\sqrt{2}}{3} r_2 E \left(\arcsin \frac{r_2}{r_3} \middle| \frac{r_3^2}{r_2^2} \right) \\ & + \frac{2\sqrt{2}}{3r_3} (r_2^2 (r_3^2 - 4)) K \left(\frac{r_2^2}{r_3^2} \right), \end{aligned} \tag{44}$$

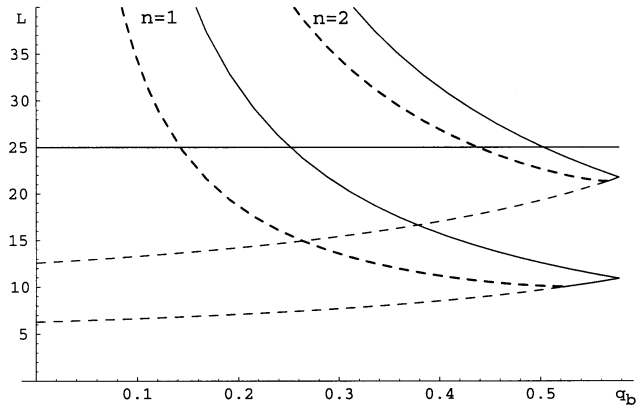
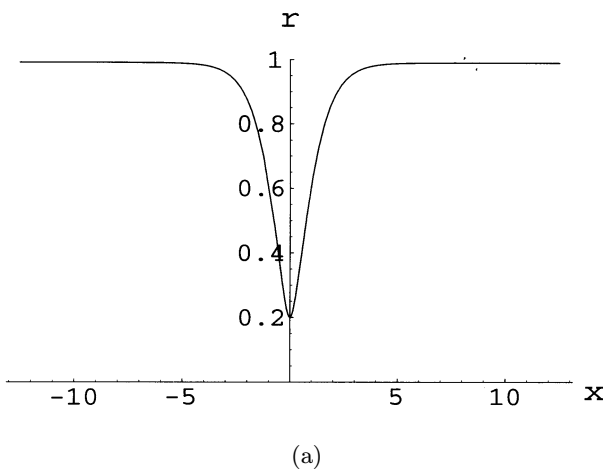


Fig. 5. Plot of L versus q_b . Solid lines stand for stable plane waves. The light dashed curves stand for unstable plane waves. The dark dashed lines represent the unstable nucleation functions.

The Lyapounov functional Φ for the homogeneous function $r = 1$ is $\Phi = -L$ and for $r = 0$ the value of Φ is 0. For the plane waves with wave number q we have

$$\Phi_q = -(1 - q^2)^2 L. \tag{45}$$

5. An Example

In this example, we fix the length of the system $L = 25$. Figure 5 shows that for this length we have two Eckhaus stable plane waves with $q_b = 2\pi/25 = 0.2513$ and $q_b = 4\pi/25 = 0.5026$. Moreover, there exist two nucleation solutions which are characterized by $n = 1$; $q_b = 0.1420$ and $n = 2$; $q_b = 0.4377$. The first one represents the saddle function between the plane waves with $n = 0$ and $n = 1$. The sec-

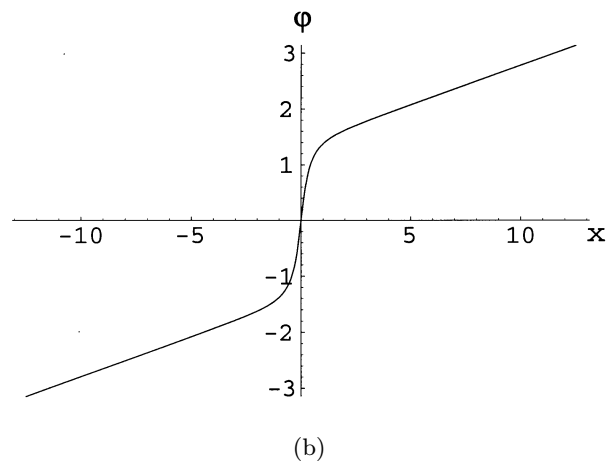
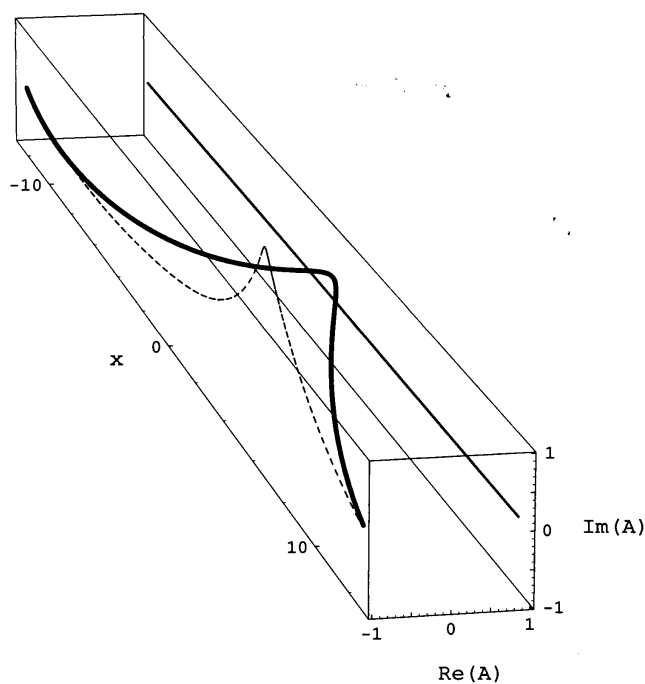
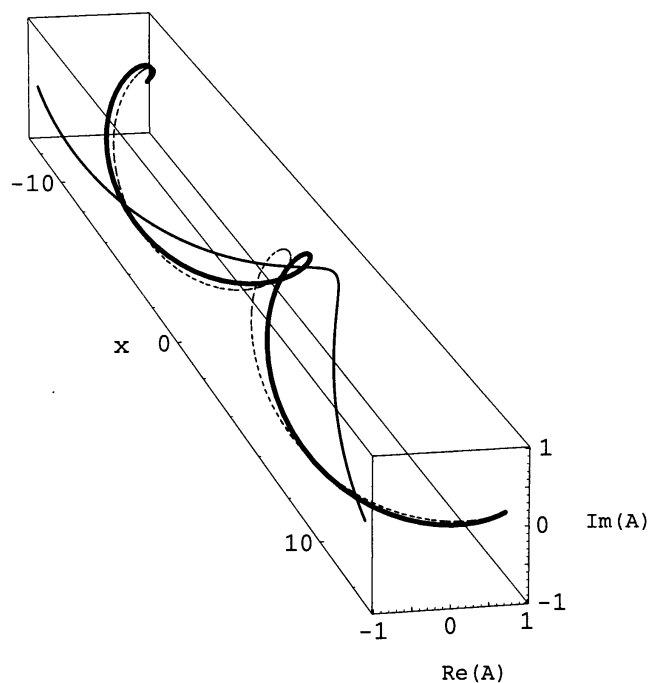


Fig. 6. (a) Module of the saddle function with $n = 1$. (b) Phase of the saddle function.



(a)



(b)

Fig. 7. (a) The dashed line is the resulting nucleation function with $n = 1$. Solid lines are for the homogeneous solution $r = 1$ and the plane wave with wave number $2\pi/L$. (b) The dashed curve represents the nucleation function between the plane waves (solid lines) with wave numbers $2\pi/L$ and $4\pi/L$.

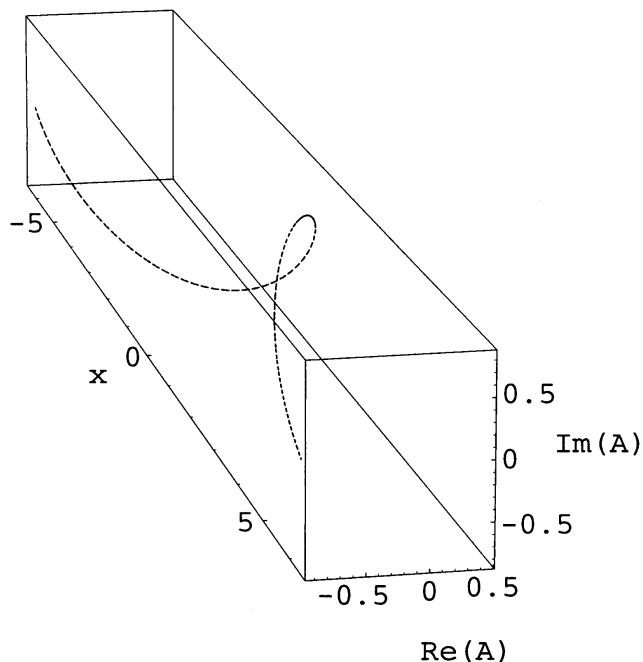


Fig. 8. The dashed line is a saddle function with phase winding number $n = 1$ and length $L = 12.5$.

and one stands for the saddle function between the plane waves with phase winding numbers $n = 1$ and $n = 2$.

Replacing these values of q_b in Eq. (18) we can determine the value of δ which in these cases gives $3.54629 \cdot 10^{-14}$ and $2.96226 \cdot 10^{-10}$, respectively. The following step is to replace the values of q_b and δ in Eq. (11). Thus the expressions for $r(x)$ and $\varphi(x)$ are completely determined from Eqs. (4) and (5). To get an impression of the shape of the nucleation functions we plot in Fig. 6 the module $r(x)$ and the phase $\varphi(x)$ for the nucleation function with phase winding number $n = 1$.

In Fig. 7 we show a 3-D view of both nucleation functions. In Fig. 7(a) the resulting nucleation function between the homogeneous solution $r = 1$ and the plane wave with wave number $2\pi/L$ is shown. In Fig. 7(b) we show the nucleation function responsible for the transition between the plane waves with wave numbers $2\pi/L$ and $4\pi/L$.

It is also possible to construct other saddle functions between the plane waves with wave numbers $2\pi/L$ and $4\pi/L$ by means of two saddle functions with phase winding number $n = 1$ and length $L = 12.5$ as shown in Fig. 8.

Moreover we can construct vortex functions according to Eq. (33). The shape of such vortex with length $L = 25$ is given in Fig. 9.

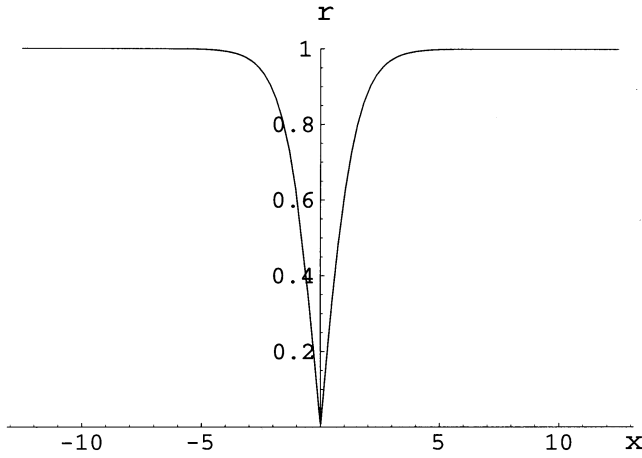


Fig. 9. Vortex function with length $L = 25$.

To compare the functions generated in this example we use the Lyapounov functional Φ . We denote by Φ_L^1 the value of the functional for the saddle function with $n = 1$ and length $L = 25$, Φ_L^2 the value of the functional for the saddle function with $n = 2$ and length $L = 25$, $\Phi_{\frac{L}{2}}^1$ the value of the functional for the saddle function with $n = 1$ and length $L = 12.5$. Moreover we denote $\Phi_{\frac{2\pi}{L}}$ and $\Phi_{\frac{4\pi}{L}}$ as the values of the potential for the plane waves with $n = 1, L = 25$ and $n = 2, L = 25$, respectively. The values for the vortex function and the homogeneous solution $r = 1$ will be Φ_L^{vor} and $\Phi_L(r = 1)$.

Using the expressions given by Eqs. (43)–(45) we obtain

$$\begin{aligned}
 2\Phi_{\frac{L}{2}}^1 &= -13.5422, \\
 \Phi_L^2 &= -13.8778, \\
 \Phi_{\frac{4\pi}{L}} &= -13.9629, \\
 \Phi_L^1 &= -20.3465, \\
 \Phi_L^{\text{vor}} &= -21.2288, \\
 \Phi_{\frac{2\pi}{L}} &= -21.9415, \\
 \Phi_L(r = 1) &= -25.
 \end{aligned}
 \tag{46}$$

6. Discussion and Conclusions

We have constructed here the nucleation solutions responsible for the transitions between the stable

plane waves of the real Ginzburg–Landau equation in a finite box.

Acknowledgments

M. Argentina would like to acknowledge the support from FONDECYT (P. 3000017). O. Descalzi wishes to thank Fondo de Ayuda a la Investigación of the U. de los Andes (P. ICIV-001-2000). E. Tirapegui acknowledges FONDECYT (P. 1990991), FONDAP (P. 11980002) and CNRS-CONICYT Project. The authors are indebted to Mr. René Rojas for many useful discussions.

References

- Elphick, C., Tirapegui, E., Brachet, M., Coulet, P. & Iooss, G. [1987] “A simple global characterization for normal forms of singular vector fields,” *Physica* **D29**, 95–127.
- Graham, R. & Tel, T. [1990] “Steady-state ensemble for the complex Ginzburg–Landau equation with weak noise,” *Phys. Rev.* **A42**, 4661–4677.
- Kramer, L. & Zimmermann, W. [1985] “On the Eckhaus instability for spatially periodic patterns,” *Physica* **D16**, 221–232.
- Langer, J. S. & Ambegaokar, V. [1967] “Intrinsic resistive transition in narrow superconducting channels,” *Phys. Rev.* **164**, 498–510.
- McCumber, D. E. & Halperin, B. I. [1970] “Time scale of intrinsic resistive fluctuations in thin superconducting wires,” *Phys. Rev.* **B1**, 1054–1070.
- Newell, A. C. & Whitehead, J. A. [1969] “Finite bandwidth, finite amplitude convection,” *J. Fluid Mech.* **38**, 279–303.
- Segel, L. A. [1969] “Distant side-walls cause slow amplitude modulations of cellular convection,” *J. Fluid Mech.* **38**, 203–224.
- Stuart, J. T. & Di Prima, R. C. [1978] “The Eckhaus and Benjamin–Feir resonance mechanisms,” *Proc. R. Soc. Lond.* **A362**, p. 27.
- Tribelsky, M. I., Kai, S. & Yamazaki, H. [1991] “Transitions between different stable states in one dimensional Ginzburg–Landau equation,” *Prog. Theor. Phys.* **86**, 963–967.
- Tuckerman, L. & Barkley, D. [1990] “Bifurcation analysis of the Eckhaus instability,” *Physica* **D46**, 57–86.